Proc. Natl. Acad. Sci. USA
Vol. 75, No. 2, pp. 828–832, February 1978
Biophysics

Drug–nucleic acid interactions: Conformational flexibility at the intercalation site

(drug intercalation/nucleotide conformation/computer model-building)

HELEN M. BERMAN*, STEPHEN NEIDLE†, AND R. KING STODOLA*

* The Institute for Cancer Research, Fox Chase, Philadelphia, Pennsylvania 19111; and † Department of Biophysics, University of London, King's College, 26-29 Drury Lane, London WC2B 5RL, United Kingdom

Communicated by Gerhart Friedlander, November 23, 1977

ABSTRACT **The conformational features of the intercalation site in polynucleotides were examined. We found that, for all the crystal structures of drug–dinucleoside complexes studied thus far, two torsion angles differ from those found in A RNA (ϕ and χ) and that alternate sugar puckering is not a prerequisite for intercalation. This intercalation geometry, which is the basis of helix axis displacement in a polymer, would necessitate conformational changes in the adjacent nucleotides. The base-turn angle is less sensitive to the conformation of the backbone than it is to small alterations in the base-pairing geometry. We postulate that this angle is dependent on the nature of the intercalating drug.**

The intercalation of drugs containing a planar chromophore with nucleic acids is considered to involve an intercalative process in which this planar group can be inserted in between adjacent base pairs of a double helix (1, 2). Two detailed categories of structural models have emerged for intercalation. In one (theoretical) model for proflavine binding, the helix axis of a polynucleotide is constrained (i.e., it remains linear) while the base pairs are stretched apart at the intercalation site, from approximately 3.4 Å to 6.8 Å separation (3, 4). This change is accomplished by alterations of the ψ and ω torsion angles (Fig. 1); there are smaller conformational changes at the adjacent nonintercalated sites. In the B DNA model there is alteration of sugar pucker at the intercalation site. In the A DNA model all the sugars retain their C3′-endo pucker. Three other models in which the helix axis is maintained have been proposed for platinum–DNA binding (5). Unwinding of these helices is measured by comparing the turn angle between successive nucleotides in the intercalated model with that of unperturbed polynucleotides.

The second category of models has been extrapolated (6) from the crystal-structure analyses of ethidium bromide–dinucleoside phosphate complexes (7–9). The important features of these crystal structures are that the helix axis kinks with a simultaneous dislocation, the sugar puckers alternate at the intercalation site, i.e., C3′-endo (3′–5′) C2′-endo, and the unwinding angle [measured in this case by comparing the angle between the C1′–C1′ vectors with that of uncomplexed dinucleoside phosphates (10, 11)] is −26°.

Most recently, a crystal structure of a cytidylyl 3′–5′ guanosine (CpG)–proflavine complex has been determined (12) which differs from previously reported structures in that it contains all C3′-endo sugars and the unwinding angle is essentially zero. [In these respects, the structure is not unlike the A DNA–proflavine theoretical model (4).] Because these structural features are apparently at variance with those of the earlier reported complexes and hence the foundations of the kinked models, we have undertaken to re-explore in some detail the conformational features of intercalated dinucleoside phosphates. In particular, we have examined the changes in conformational angles upon intercalation, as well as the structural features that affect the relative orientations of the base pairs.

The costs of publication of this article were defrayed in part by the payment of page charges. This article must therefore be hereby marked "*advertisement*" in accordance with 18 U. S. C. §1734 solely to indicate this fact.

METHODS

A molecule of CpG with an A RNA conformation (13, 14) was chosen as the starting model because the available crystal structure data have been derived from ribodinucleoside phosphate complexes. An interactive graphics program implemented on a PDP11/40 with a Vector General graphics display system was used to compose from the coordinates of the dinucleoside phosphate (C_0) two strands (C_1 and C_2) related by 2-fold symmetry:

$$C_1 = RC_0 + r$$

$$C_2 = S(RC_0 + r).$$

S is the 2-fold rotation matrix across the y axis; R is an orthogonal rotation matrix derived from three angles (α_x, α_y, and α_z), and r is a translation vector of three parameters (d_x, d_y, and d_z). Varying these six parameters allowed the two strands to be oriented in any fashion while 2-fold symmetry was maintained. [For the purposes of this experiment, exact symmetry was imposed although the duplex can be asymmetric.] Changes were made in the original coordinate set, C_0, by modifying the torsion angles. Initial values for the six parameters were obtained and modified by minimizing a function that reflects the deviation from a base-paired configuration (10, 11, 15). This function is of the form:

$$\sum_{i=1}^{N_{data}} \left(\frac{a_i - \hat{a}_i}{w_i}\right)^2 + \sum_{j=1}^{N_{constraints}} q \times [\max(\hat{c}_j - H_j, 0) + \max(L_j - \hat{c}_j, 0)]^2$$

N_{data} is the number of data points (i.e., distances, torsion angles, bond angles, and dihedral angles between planes); $N_{constraints}$ is the number of constraints; the $\hat{a}_i$ are the observed distances, torsion angles, bond angles, and dihedral angles between base planes; the $\hat{c}_j$ are the observed distances, angles, etc., derived from coordinates in the strands C_1 and C_2 as modified by α_x, α_y, α_z, d_x, d_y, and d_z; a_i are the midpoint of acceptable range of distances, angles, torsion angles, and plane angles; the w_i are the weights for the observations; L_j is the lowest value $\hat{c}_j$ should take; H_j is the highest value $\hat{c}_j$ should take; and q is a constant chosen to satisfy properties *ii* and *iii* below. The purpose of the function in the rightmost sum is to provide a continuously differentiable function with the following properties:

(*i*) It is zero when $L_j \leq \hat{c}_j \leq H_j$, and
(*ii*) it is large (relative to the left sum) when $\hat{c}_j < L_j$ or $\hat{c}_j > H_j$ and
(*iii*) it is not so large as to "overwhelm" the minimization.

This error function was minimized by using Marquardt's algorithm (16). Structures with small residual errors and good base-pair geometry were accepted; that is, the hydrogen-bonding distances ranged between 2.7 and 3.0 Å, the angles between 105° and 130°, and the dihedral angles between base planes between 0° and 20° (15).

The six parameters controlling relative orientation were also changed by using control dials. This was useful for allowing optimization to begin from different initial orientations. Because the functions sometimes had several local minima, this occasionally led to different but equally acceptable results.

RESULTS

Examination of the crystal structures of the dinucleoside phosphate–drug complexes studied to date (7–9, 12) shows that the two major conformational deviations from A RNA are in the bond rotations designated as ϕ and χ (Fig. 1). From the conformation of A RNA as a starting model (Fig. 2*a*), an acceptable intercalation geometry was produced on the graphics display by changing these two angles. When the angle about C5′–O5′ (ϕ) is increased by about 50° from its value of 175° in A RNA (Table 1), the backbone extends and the base pairs break. The increase in the glycosidic χ angle of the base at the 3′ end (i.e., the guanine in CpG) by 60° from its normal value of 13° allows the bases to become parallel again, and thus the base pairs to be reformed (Fig. 2*c*). In an actual duplex, ϕ and χ would increase concurrently, stretching the spacing while maintaining base pairing (Fig. 2*b*). Fig. 2*b* shows a structure with values of χ and ϕ midway between those of A RNA and an intercalated model. The intercalated model shown in Fig. 2*c* corresponds closely to the structure found for the proflavine–CpG complex (12). To understand the effect of this geometry if it were to be found in a polynucleotide, consider the orientation of the ribose sugar oxygen as defined by a vector between the center of the C2′—C3′ bond and the O1′ oxygen atom (17). In a helical nucleic acid the vectors in each strand are parallel to one another. At the intercalation site these vectors

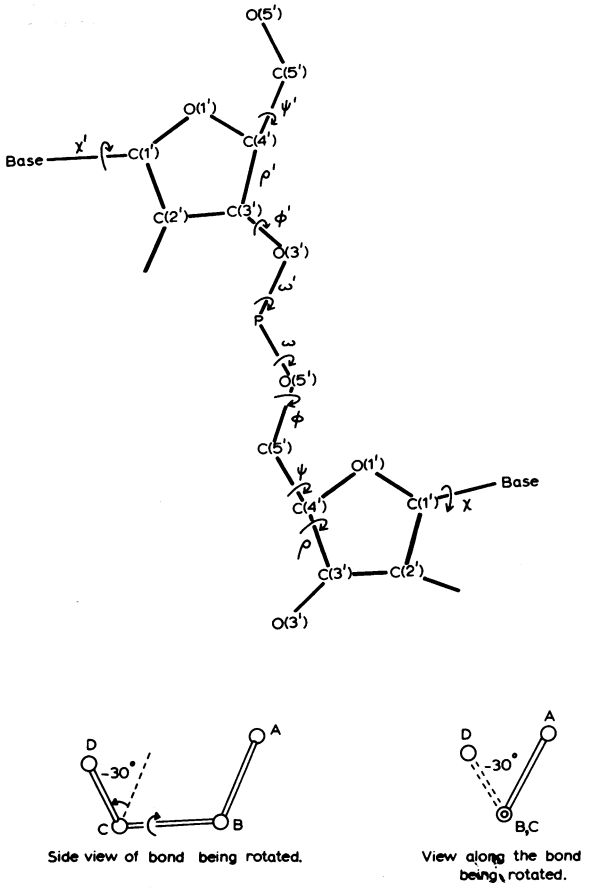

FIG. 1. Conformational nomenclature for the nucleoside backbone.

Table 1. Structural features of intercalated dinucleoside phosphates

Structure	Conformation angles, degrees χ	χ'	ϕ	ϕ'	ω	ω'	ψ	Pucker 3′ → 5′	Base twist*, degrees	Base turn†, degrees
Hypothetical models										
Fig. 4*a*	80	13	225	213	300	281	50	C3′endo,C3′endo	10	15
Fig. 4*b*	80	13	225	213	300	281	50	C3′endo,C3′endo	4	27
Fig. 4*c*	95	13	230	220	300	280	70	C3′endo,C2′endo	16	11
Fig. 4*d*	95	13	235	210	280	300	70	C3′endo,C2′endo	15	25
Experimental models‡										
CpG–proflavine (12)	85(+72)	17(+4)	231(+56)	201(−12)	289(−11)	290(+9)	52(+2)	C3′endo,C3′endo		
i^5-UpA–ethidium bromide (7)	99(+86) 100(+87)	26(+13) 14(+1)	236(+61) 230(+55)	207(−6) 218(+5)	291(−9) 276(−24)	286(+5) 302(+21)	52(+2) 70(+20)	C3′endo,C2′endo		
i^5-CpG–ethidium bromide (8)	101(+88) 109(+96)	29(+16) 24(+11)	210(+35) 224(+49)	226(+13) 225(+12)	286(−14) 291(−9)	281(0) 291(+10)	72(+22) 55(+5)	C3′endo,C2′endo		
Polynucleic acids										
A RNA (14)	13	13	175	213	300	281	50	All C3′endo		
A DNA (14)	26	26	210	178	275	313	45	All C3′endo		
B DNA (14)	85	85	209	159	321	261	31	All C2′endo		
A DNA–proflavine (4)	23	23	212	211	201	261	149	All C3′endo		

* The base twist angle is defined as the dihedral angle between base planes in a base pair.
† The base turn angle is the angle between the vectors connecting the C1′ atoms of each base pair when projected on the average base plane viewed from a point perpendicular to this plane.
‡ Numbers in parentheses are deviations from A RNA.

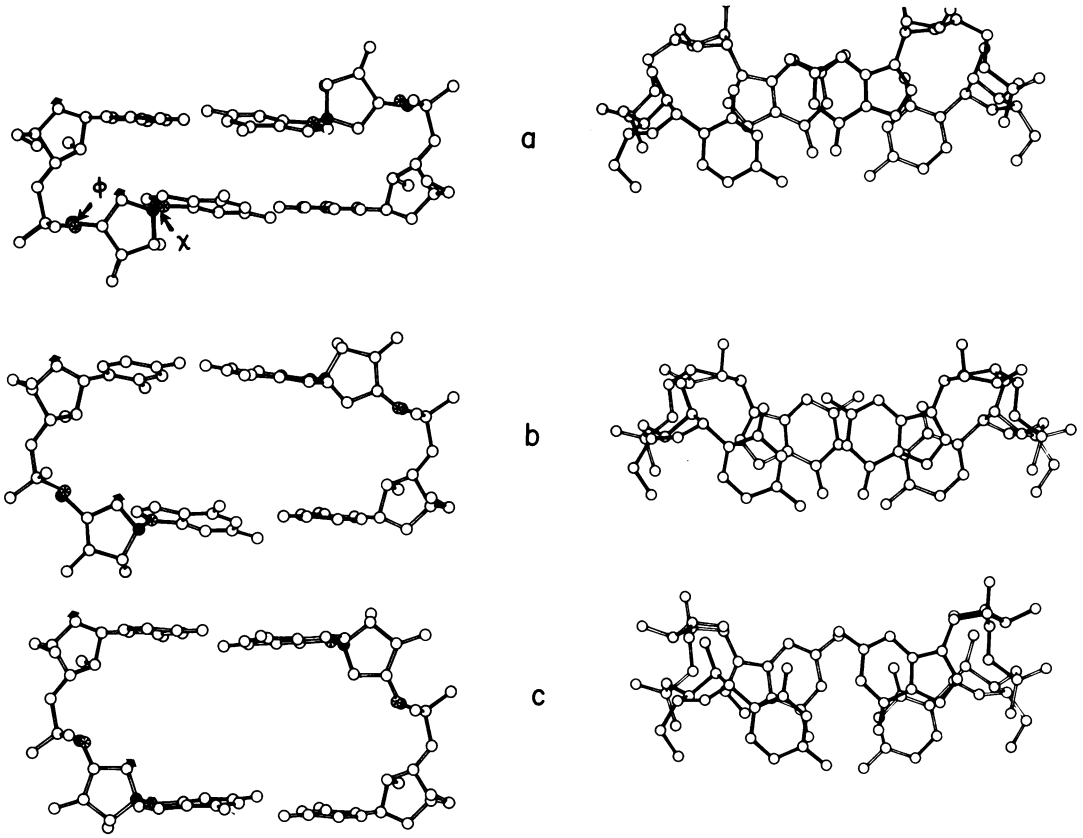

FIG. 2. Stepwise description of the stretching of a dinucleoside phosphate (CpG). (*a*) A RNA conformation; (*b*) A RNA with an increase in $\phi = 200°$, $\chi = 45°$; (*c*) a possible intercalation geometry $\phi = 225°$, $\chi = 80°$. (*Left*) Views parallel to the base planes; (*Right*) views approximately perpendicular to the base-pair planes. The arrows represent the vector between the center of the C2′—C3′ bond and the O1′ atom.

are skew to one another and cause a disruption in the helix. The overlap of the bases is also altered by these conformational changes such that when viewed perpendicular to the base pair planes, the front base pair (in this case cytosine-guanine) slides to the right and the back base pair to the left of what is found in A RNA.

Because it has been demonstrated experimentally that the sugar puckers in the dinucleoside complexes can be either mixed (7–9) or the same (12), we have attempted to determine the nature of the structural changes that may be produced when the pucker is changed. The RNA model was altered to a C3′-endo, C2′-endo geometry, and the ϕ and χ angles were increased. At least nine acceptable base-paired structures were obtained with additional small changes in the other backbone angles. One example is shown in Table 1 and Fig. 3. This structure is similar to that of CpG–proflavine in that the ribose sugars of this structure are skew to one another with only minor differences in the base overlap. On this basis, successive sugars in the intercalated complex can be of either identical or mixed pucker.

The effects of small (<20°) changes in the other backbone angles were examined. One probe of gross structure that we used is the angle between the vectors connecting the C1′ atoms of each base pair when projected on the average base plane viewed from a point perpendicular to this plane. Rather than regarding this as a measure of unwinding of a polymer, we shall refer to this as the base turn angle B since we are dealing only with a dinucleoside. The backbone angles were altered over a 20° range. As shown in Fig. 4 and Table 1, it is possible to generate structures that have different B angles and yet small (or no) differences in the backbone conformational angles. Changes in the B angle are sometimes accompanied by small changes in the hydrogen-bonding geometry such that, for example, in one case the base pair has a 4° twist and in another there is a 10° twist (Table 1). Several acceptable geometries were generated in this way.

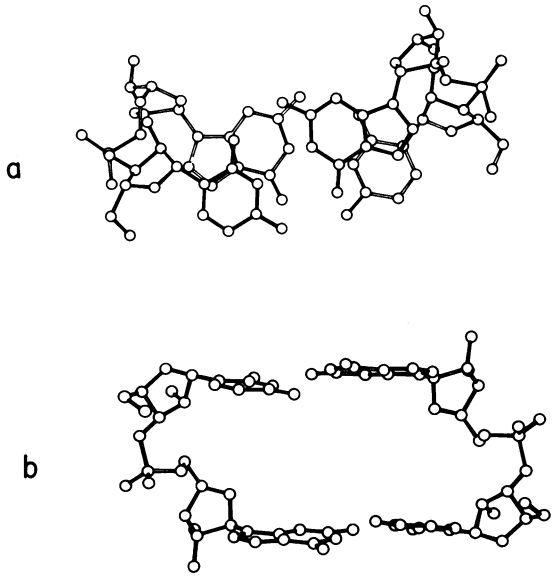

FIG. 3. An intercalated dinucleoside with C3′-endo, C2′-endo sugar pucker viewed (*a*) perpendicular and (*b*) parallel to the base plane.

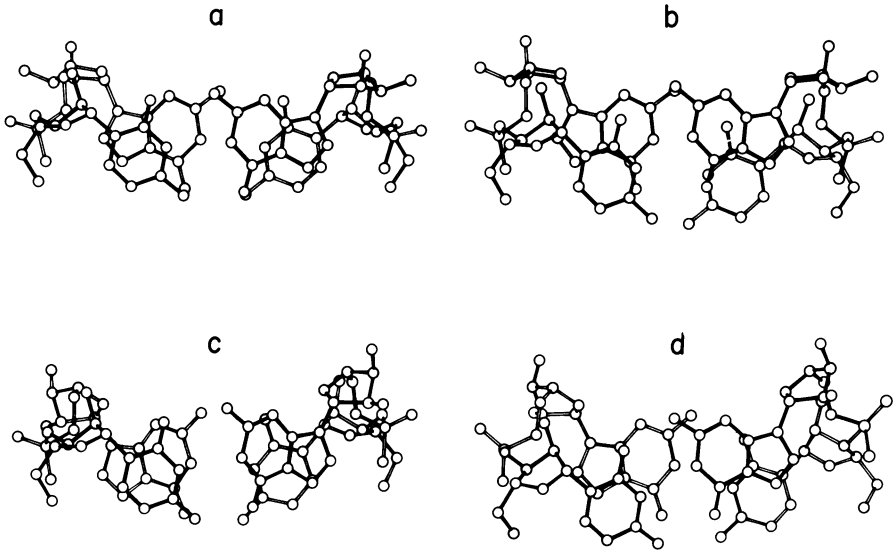

FIG. 4. Examples of intercalation geometries with different B angles. Views are approximately perpendicular to the base planes. (*a*) C3′-endo, C3′-endo small B angle; (*b*) C3′-endo, C3′-endo large B angle. There are no conformational differences between the nucleotide backbones. There are changes in the association between two strands. (*c*) C3′-endo, C2′-endo small B angle; (*d*) C3′-endo, C2′-endo large B angle. There are small conformational differences between *c* and *d*. See Table 1.

DISCUSSION

We have examined the conformational features of intercalated dinucleoside phosphates and have observed that it is possible to construct models where only two conformational angles differ significantly from those found in A RNA (ϕ and χ). We have also observed that the sugar pucker does not seem to be an important feature of the intercalated dinucleoside phosphate. In a qualitative sense, the altered ϕ and χ angles may be described as *trans* and *anti*, respectively, and they thus conform to the "rigid" nucleotide descriptions (18). However, the fine tuning of these angles leads to structures at the intercalation site that deviate markedly from the helical dinucleotide building blocks of RNA. [The same effect is achieved in A DNA by increasing χ by about 60° and each of the other backbone angles by less than 25° (Table 1).]

To summarize, in this intercalation geometry, (*i*) the helicity is disrupted, as evidenced by the skewed ribose rings; (*ii*) the base overlap is different; and (*iii*) the nucleoside groups are asymmetric—a guanine with a high χ angle is base paired to a cytosine with a low χ angle. The consequences of these features are that, in a polymer, the conformations of the *adjacent* nucleotides possibly extending beyond more than one on either side must be adjusted in order to relieve the steric strain caused by the asymmetry and the changes in base overlap. For example, to fit the intercalation geometry shown in Fig. 2 into A RNA ($\chi = 14°$) requires considerable distortion at the adjacent sites, and preliminary model building shows that ω and ψ of the nucleotide adjacent to the guanine must be changed by large amounts; the other angles are altered to a lesser degree. The presence of the O2′ hydroxyl compounds the difficulty. Because the base overlaps of the intercalated structures shown in Fig. 4 are similar to that found in B DNA ($\chi = 85°$), it is somewhat easier to fit those models with *either* C3′endo, C2′endo or C3′endo, C3′endo sugar puckers into B DNA than it is into RNA. In this case conformational adjustments must be made to the residue adjacent to the cytosine in order to relieve the steric strain carried by the asymmetry of the χ angles. The nature of the adjustments to the sites adjacent to the guanine depends on the sugar pucker.

Our models, in combination with the experimental models (7–9, 12), indicate that there is a continuum of stereochemically plausible opened-up dinucleoside phosphate structures; we have examined only some of the many possible structures and have presented a few of those. The question arises as to why different intercalation geometries have been observed: the base-turn angle in the ethidium bromide–UpA and CpG complexes is about 8° (7, 8), whereas the proflavine—CpG complex has a B angle of about 33° (12). [A recent report of a second proflavine–CpG complex suggests that the crystal contains a duplex with a small B angle (19)]. It seems that there is a simple rationale for these observations, which becomes apparent when the structure of the drug itself is taken into account. Ethidium bromide (Fig. 5) is a bulky molecule with both phenyl and ethyl substituents. Such a molecule could not be accommodated in an intercalated dinucleoside phosphate with a large B angle, such as in Fig. 4*b*, because of unfavorable van der Waal's contacts. A structure with a small B, such as in Fig. 4 *a* and *c* would not produce these unfavorable interactions, and not unexpectedly, the structure in Fig. 4*c* is close to that found experimentally. On the other hand, proflavine, with its lack of substituent on the middle ring, might be expected to intercalate into a structure with either a large or small B angle without producing unacceptable interactions, as indeed is found. This principle, of the base-turn angle being dependent upon the size

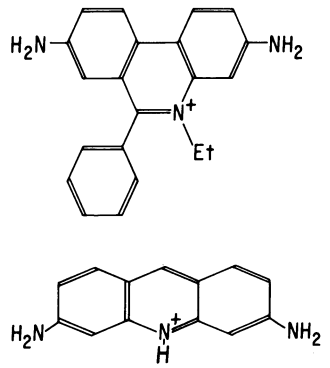

FIG. 5. The chemical formulas of (*Upper*) ethidium bromide and (*Lower*) proflavine.

of the intercalated drug molecule, is a plausible one for polynucleotides as well as their oligomers.

This work was supported by U.S. Public Health Service Grants GM 21589, CA 06927, and RR05539 from the National Institutes of Health, by an appropriation from the Commonwealth of Pennsylvania, and by a grant from the Cancer Research Campaign.

1. Lerman, L. S. (1961) *J. Mol. Biol.* **3,** 18–30.
2. Gale, E. F., Cundliffe, E., Reynolds, P. E., Richmond, M. H. & Waring, M. J. (1972) *The Molecular Basis of Antibiotic Action* (John Wiley, London).
3. Alden, C. J. & Arnott, S. (1975) *Nucleic Acids Res.* **2,** 1701–1717.
4. Alden, C. J. & Arnott, S. (1977), *Nucleic Acids Res.* **4,** 3855–3861.
5. Bond, P. J., Langridge, R., Jennett, K. W. & Lippard, S. J. (1975) *Proc. Natl. Acad. Sci. USA* **72,** 4825–4829.
6. Sobell, H. M., Tsai, C. C., Jain, S. C. & Gilbert, S. G. (1977) *J. Mol. Biol.* **114,** 333–365.
7. Tsai, C. C., Jain, S. C. & Sobell, H. M. (1977) *J. Mol. Biol.* **114,** 301–315.
8. Jain, S. C., Tsai, C. C. & Sobell, H. M. (1977) *J. Mol. Biol.* **114,** 317–331.
9. Tsai, C. C., Jain, S. C. & Sobell, H. M. (1975) *Proc. Natl. Acad. Sci. USA* **72,** 628–632.
10. Rosenberg, J. M., Seeman, N. C., Day, R. O. & Rich, A. (1976) *J. Mol. Biol.* **104,** 145–167.
11. Seeman, N. C., Rosenberg, J. M., Suddath, F. L., Kim, J. J. P. & Rich, A. (1976) *J. Mol. Biol.* **104,** 109–144.
12. Neidle, S., Achari, A., Taylor, G. L., Berman, H. M., Carrell, H. L., Glusker, J. P. & Stallings, W. C. (1977) *Nature* **269,** 304–307.
13. Arnott, S., Dover, S. D. & Wonacott, A. J. (1969) *Acta Crystallogr. Sect. B* **25,** 2192–2206.
14. Arnott, S., Smith, P. J. C. & Chandrasekaran, R. (1976) in *Handbook of Biochemistry and Molecular Biology,* ed. Fasman, G. D. (Chemical Rubber Co., Cleveland, Ohio), 3rd Ed., Vol. 2, Sect. B. pp. 411–422.
15. Voet, D. & Rich, A. (1970) *Prog. Nucleic Acid Res. Mol. Biol.* **10,** 183–265.
16. Marquardt, D. W. (1963) *J. Soc. Ind. Appl. Math.* **11,** 431–441.
17. Kim, S. H., Berman, H., Sussman, J. L. & Newton M. (1973) *Acta Crystallogr. Sect. B* **25,** 703–710.
18. Yathindra, N. & Sundaralingam, M. (1973) *Biopolymers* **12,** 297–314.
19. Seshadri, T. P., Sakore, T. D. & Sobell, H. M. (1977) *American Crystallographic Association Abstr.* **5,** no. 2, N5.